RSC Advances

ROYAL SOCIETY OF CHEMISTRY

www.rsc.org/advances

Ab initio simulations of defect-based magnetism: The case of CoSi nanowires

Tai-Kang Liu[1], Shan-Haw Chiou[2], Johan van Lierop[3*] and Chuenhou (Hao) Ouyang[1*]

[1] Department of Materials Science and Engineering, National Tsing Hua University, Hsinchu, Taiwan 300, Republic of China

[2]Material and Chemical Research Laboratories and Nanotechnology Research Center, Industrial Technology Research Institute, Hsinchu, Taiwan 310, Republic of China

[3]Department of Physics and Astronomy, University of Manitoba, Winnipeg, MB, R3T 2N2, Canada

[1*] houyang@mx.mthu.edu.tw

[3*] Johan.van.Lierop@umanitoba.ca

Abstract

The source of the unusual ferromagnetism of nanowires (NWs) such as CoSi-SiO_2 has been studied by first-principles calculations. While previous experiments on ferromagnetic NWs presumed that their magnetism was the result of metal ions at the interface suffering reduced coordination, first-principles calculations of such a configuration revealed that this would only account for ~20% of the measured magnetization. Selected area electron diffraction (SAED) transmission electron microscopy (TEM) diffraction patterns collected in the metal interface region indicated that a superlattice structure was present, contrary to the bulk. We take the case of CoSi-SiO_2 NWs, and using simulated diffraction patterns, verify the CoSi ordered vacancies superstructure interpretation of experiment. With first principles simulations, once the ordered vacancies are incorporated with interface Co atoms, the resulting simulations result in a ~97% agreement with the experimental magnetization.

Our results clearly indicate that these internal, ordered vacancies in NWs are the dominant mechanism for the observed ferromagnetism. Density of states calculations show that as the metal atom's coordination inside the ordered vacancies structures increase, the overall magnetization decreases. For CoSi nanowires, the variations of the Co moments at different sites depend on the vacancy configuration, which can be understood through the effects of the bond lengths on Co atom's moments. According to the Bethe-Slater curve, there is a requisite bond length range for the presence of enough exchange energy to permit ferromagnetism. We find that this bond length plays a crucial role in setting the distribution of Co moments about the vacancies.

Introduction

The magnetism of nanoscale systems is extremely sensitive to small changes in size, structure, and composition, normally due to surface and interface properties playing a particularly important role. This work intends to examine factors that can induce magnetism beyond surface and interface effects. For example, recent observations of unexpected ferromagnetism arising from quantum confinement effects in systems that are not ferromagnetic in the bulk [1-5]. One of the more intriguing systems are nanowires made with transition metal-based monosilicides such as CoSi [1]. Not only are single-phased nanowire structures formed, but an interface layer of SiO_2 covers the nanowires due to vapour reaction and metal diffusion during synthesis. The Si and SiO_2 molecules provide different environments for the metal ions, and are the likely origin of the ferromagnetism. [6,7] Nanowires are formed typically using a straightforward modification of the van Arkel method [8] where the nanowires form via a vapour-solid growth mechanism [9] (e.g. how K. Seo et al.[1] made CoSi nanowires), with Ar gas used as a carrier that transports a metal-chloride vapour onto a Si substrate. The metal chloride decomposes and reacts with the Si to form free-standing nanowires. The formation of interface SiO_2 on the nanowires occurs through metal diffusion [10] during oxidation, where the silicide decomposes at the silicide/oxide interface, providing Si for oxidation followed by the free metal

diffusing to the underlying Si, forming more silicide. For CoSi nanowires, $2CoCl_2$ (g) + 3Si (s) ⇔ 2CoSi (s) + $SiCl_4$ (g) is followed by CoSi (s) + O_2 (g) ⇔ Co(s) + SiO_2 (s) and Co (s) + Si (s) ⇔ CoSi (s) is the accepted reaction pathway.

Experiments, calculations and simulations

The analyses of transmission electron microscopy (TEM) images was based on Multislice simulations [11]. The ab initio simulations used the Vienna ab initio simulation package (VASP), which is based on first principles density functional theory (DFT) using the generalized gradient approximation (GGA) - k points: 2×4×1 [12, 13] and the energy convergence condition is less than 10^{-3} eV. The self-consistent total ground-state energy of the system for any set of Co ion positions was determined using a conjugate gradients iterative minimization technique. Additionally, this plane-wave formalism produced the Hellmann-Feynman forces [12] that were used for the ab initio relaxation of the ionic positions until residual forces on individual atom were less than 0.5 eV/Å [6,7,14,15]. This average drift force less than 0.5 eV/Å per atom (mainly around the interface) has been used before [16], where those simulations provided a ~90% agreement with experiment. In this work, details of magnetization for individual atom are discussed using tighter and more exact convergence settings, which (in principle) should be more reliable when one judges agreement with experiment, and more accurate for individual atomic magnetizations.

Results and Discussions

For CoSi nanowires, TEM analysis identified epitaxial crystalline growth [1]. The

high-contrast component of electron diffraction patterns indicated that the CoSi structure was the same simple cubic B20 space group used to describe the structure of bulk CoSi. However, the lower-contrast components of a pattern revealed that there was a superstructure with a period twice that of the bulk lattice constant. These low contrast components (i.e. the weaker spots in the electron diffraction images) were present everywhere along the nanowires, and could be due to either anisotropic growth or periodic ordered vacancies in some of the crystallographic sites. In keeping with these observations, we modelled the B20 structure of CoSi along all three axes with specific Si sites removed using Multislice software, as shown in Figure 1. The simulated diffraction pattern compares well with the TEM SAED (selected area electron diffraction) experimental results.

The question that follows is are these ordered vacancies the origin of observed ferromagnetism, in a way similar to defect-based magnetism observed in nanoparticles and thin films [17]. Or, do they at least influence the observed ferromagnetism in the nanowires? Bulk forms of the nanowire compositions are typically diamagnetic (as is the case for CoSi [18]), while the nanowires are ferromagnetic. This behaviour indicates that the bonding conditions around the metal atoms are the key to the understanding the observed magnetization. Asymmetrical bonding near and around interfaces could be one possible origin of the ferromagnetism. [6] In general, the strongly interacting spin-exchange pathways between metal ions of a magnetic solid are determined through the overlap of their orbitals.[19] Therefore, the bond lengths of the metal atoms surrounded by different coordination environments may cause fluctuations of the exchange that result in an observed ferromagnetic magnetization.

CoSi nanowires present a room-temperature *M(H)* hysteresis loop with nonzero remnant magnetization and coercivity[1]. *M(H)* loops with essentially the same field dependencies were observed down to 2 K, with only a weak increase in the measured saturation magnetization. At first, this observed ferromagnetic-like behavior was attributed to changes in electronic structure of the Co atoms via interface ligand interactions affecting crystal fields. The most straightforward explanation with the information at hand was that the observed ferromagnetism was simply due to uncompensated Co spins and their reduced coordination at the nanowire surface (keep in mind that the surface-to-volume ratio is high for nanowires). We have undertaken first principles calculations following these reasonable assumptions, and our simulations of the magnetism of such a CoSi nanowire structure indicates that the average moment of Co atoms near the surface/interface are $0.3526\mu_B$, significantly less than the magnetometry determined $0.84\mu_B$ /Co atom. [7] It would seem that it is unlikely that the ferromagnetism could be solely from reduced coordination of Co ions. It is possible that ordered vacancies in a CoSi nanowire provide a reduced coordination, and we try and resolve the contribution of ordered vacancies to the measured magnetization from that of interfacial bonding enhanced moments, and ascertain the sources of the nanowire magnetization.

Selected area diffraction images of nanowires from TEM analysis that present ordered vacancies also occurred in $ErSi_{2-x}$ nanowires [20] where the weaker extra diffraction spots not present in the parent bulk structure images were observed. A superlattice spot distribution along the c-axis identified ordered vacancies in the Si lattice positions, reducing the compressive stress between the Si bonds. The source of the stress may come from volume shrinkage during the silicide formation of the nanowires. Due to Si's small atomic density, silicide reactions are often

accompanied reduced volume (about 22% in CoSi), causing a compressive stress.[21] Stress from lattice mismatch may also be present; rare-earth silicide and the silicon substrate increase lattice constants by 6.4~7.8% at room temperature [22]. Finally, during the reaction process expansion of nanowires and substrate will provide a heat induced stress (expansion coefficient of CoSi is $11.1\times10^{-6}K^{-1}$ at room temperature [23] - three times that of Si at $3\times10^{-6}K^{-1}$). The simulations used the relaxation displacement model [24] to incorporate the above effects, where only the nearest-neighbor interactions were considered since aligned pairs of vacancies have lower energy than a single vacancies.

For the simulations that provide a measure of the Co moments in the (epitaxial) CoSi nanowires, the $P2_13$ space group (consistent with the bulk cubic B20 type structure) with a lattice constant of 4.438 Å [3] was used. To begin, the band structure [25] and the density of states (DOS) of bulk CoSi was calculated (Figure 2) [26] and it presents the expected semimetal character. Next, the effects of the superlattice structure in the nanowires with twice the lattice constant of cubic CoSi, was investigated. We have calculated the magnetization of both the CoSi-SiO_2 nanowires with and without ordered vacancies in order to examine the effects of the vacancies, as shown in Figures 3 and 4. SiO_2 enclosing the CoSi nanowires (CoSi-SiO_2 nanowires, Figure 3) is a result of the sample preparation of the CoSi on a Si substrate combined with the formation of a native oxide [1]. Evidence of this SiO_2 phase was present in low magnification TEM images via charging effects, and an amorphous region enveloping the crystalline CoSi nanowires was observed clearly in the higher magnification images [1,27,28]. The model structures described below included the amorphous SiO_2 component of the nanowire structures and the SiO_2's influence on the vacancies.

The structurally ordered vacancy configuration in the CoSi nanowires may be induced by their anisotropic growth, or periodic vacancies at some of the crystallographic sites. To simulate the possible impact on the magnetism, vacancies were positioned with twice the lattice constant, linking Co ions to the substrate. As nanowires grow along the [211] direction (based on TEM analysis [1]) and are covered with amorphous SiO_2, the $[\bar{1}02]$ side direction of CoSi attached to SiO_2 was used (Figure 4). A CoSi supercell was made with 160 Co and 136 Si atoms whose length, width and height was 19.847 Å, 8.876 Å and 19.847 Å, respectively. The SiO_2 supercell was made with 53 Si and 115 O atoms with length19.847 Å, width 8.876 Å and height 15 Å; for the amorphous SiO_2 component, atomic positions were chosen following the work of R. J. Bell et al.[29] Once the nanowire core and shell structures were established, relaxation under the free lattice constants condition was applied. The magnetization of CoSi-SiO_2 nanowires could then be determined, as shown in Figure 4.

Keeping the above considerations in mind, a simulation of CoSi nanowires on SiO_2 without ordered vacancies in the CoSi was performed first. The average moment of Co atoms from every plane parallel to the interface compared to the distance to the interface, and the associated supercell used for the simulations of structure, are shown in Figure 4. Approximately 1.47% of the Co atoms are on the interface of the CoSi [1], using the measured distribution of nanowire diameters (20 nm) combined with the roughness between the CoSi and amorphous SiO_2. Setting a Co interface atom down to an interfacial depth of 2.2 Å identified the average moment per internal Co atom to be $0.0027\mu_B$/atom. The simulation shows that disregarding the interface effects on the nanowires, the internal Co atoms should be essentially diamagnetic. With the

incorporation of both interface and internal Co atoms to the nanowire magnetization, the total Co moment was only increased to 0.1638μ_B/atom. This calculation showed that the dangling bonds around the interface can only contribute a fraction of the total magnetization. Without the ordered vacancies internal to the nanowires, the moment per Co atom is far below the experimental value. (consistent with results from GGA+U presented in Supplemental Materials/Fig. S1 and S2) To explore the relationship between the bonding environment and the magnetization, three different Co site configurations were examined (Supplemental Materials/Fig. S3). The internal atom 1 coordinated with seven Si atoms, which is inside the matrix, provides no magnetization, with the spin-up and spin-down DOS quite symmetric. The internal atom 2, which is closer to the interface, coordinates with six Si atoms, but the resultant magnetization only increases to a few $10^{-3}\mu_B$; the internal Co atoms cannot be the origin of the observed magnetization. The likely source of the measured magnetization is from Co atoms at the interface. Co atom 3, which coordinates with three Si atoms and right on the interface, yields a calculated magnetization of 0.4800μ_B. Clearly, the model without ordered vacancies fails to map onto the experiments.

The effects of ordered vacancies in the CoSi nanowires were incorporated. Average moments of Co atoms from every plane parallel to the interface as a function of the distance to the interface, and the associated supercell used for the simulations of structure (with ordered vacancies), are shown in Figure 4. With the previous system conditions described above, first-principles calculations indicate the average moment per interface Co atom is 0.3611μ_B/atom. This improves the difference between simulation and experiment to approximately 57% [1]. From the simulations we find that surface component of the magnetization goes from 0.1611 μ_B/Co atom to 0.3611

μ_B/Co atom when incorporating the effects of ordered vacancies and defects. The internal nanowire magnetization changes from essentially diamagnetic (0.0027 μ_B/Co atom to 0.8074 μ_B/Co atom. Combining the effects of ordered vacancies with the internal Co nanowire magnetization, the overall Co moment becomes $0.8074\mu_B$, in good agreement with the experimental result of $0.8400\mu_B$ (within 4%). The results of the simulations show that the moments of interface and internal nanowire Co atoms contribution to the total magnetization is largely due to ordered vacancies. Again, we choose three different Co sites to discuss the relationship between the bonding environment and the results on the magnetization (Supplemental Materials/Fig. S4). The internal atom 1' coordinated with six Si atoms, which resides inside the matrix, yields a nearly zero magnetization again, and the spin-up and spin-down DOS are symmetric. The internal atom 2' that is closer to the interface, coordinates with six Si atoms, and the overall magnetization increases to $0.1700\mu_B$. The internal Co atoms closer to the interface supply more magnetization to the CoSi nanowires than the ones in the structure without ordered vacancies. The density of states within the matrix becomes less symmetric compared to those of the system without vacancies. Atom 3' coordinated with four Si atoms, which is at the interface, yields a magnetization value of $0.8830\mu_B$. The Bader charge [30,31,32,33,34] of a Co atom in a CoSi-SiO2 core-shell nanowire further indicates that there is a difference between spin up and spin down electron densities (↑-↓, obtained by means of spin-polarized and GGA simulations within VASP a for single k-point and total drift force less than 0.17 eV/Å). The Bader charges for 2' Co site layer average is 0.137e higher the average Bader charges 1' Co site layer 0.004e (Supplemental Materials/Fig. S5 and S6). This result is consistent with the magnetic moment calculated directly with VASP. The contour of ↑-↓ spin electron densities about the 2' atom layer and 1' atom layer illustrates that the 2'atom layer has more spin polarized magnetic moments.

In both cases, simulations show that the poor (or low) coordination number around the metal atoms results in a higher magnetization. A similar trend resulted from first principles simulations of bulk $MnSi_x$ (x=1.73~1.75) [35] where the average magnetic moment per Mn ion was almost four times greater than the stoichiometric MnSi; this enhancement was due to the variation of Mn ion coordination, where higher coordination ions suffered quenched moments. The coordination of Mn and its effect on the magnetism varies with the group element, as Mn doping in amorphous Si and Ge has shown. [36]

The effects on the internal Co atoms from different coordination are shown in Figure 5. The internal Co atoms without ordered vacancies coordinate with seven Si atoms, and the average magnetization is nearly zero. The coordination number of Co atoms with ordered vacancies varies from five to seven, and the average magnetization of low coordination number Co atoms is higher than that of higher coordination, due to the uncompensated electrons around the atoms. However, there is fluctuation amongst individual atoms as simulations indicate that some Co atoms with low coordination number may yield a negative magnetization value (i.e. counter-aligned spins). This may be explained by the physics behind the Bethe-Slater curve [37], where ferromagnetism depends strongly on the bond length: Only atoms within a certain bond length range have the necessary positive exchange energy to induce ferromagnetism.

Conclusion

In summary, ferromagnetism for nanowires is found to be from interface and internal

metal atoms, where for the case of CoSi nanowires, the average moment per Co atom around the interface 0.3611μ_B/atom, and internal nanowire magnetization $1.8862\times10^{-3}\mu_B/Å^3$. These results are consistent with those using a LDA+U method, as presented in the Supplemental Materials. The experimental results indicated an average Co moment around the interface to be 0.8400μ_B/atom, while our simulation results indicate interface and internal moment values for interface Co atoms to be 0.8074μ_B/atom. In addition to the asymmetrical bonds of metal atoms with Si or O atoms around the interface contribution to the ferromagnetism, asymmetric bonding caused by internal vacancies also contributes. We find that the coordination number and the bond length with metal ions combined with local spatial fluctuations are responsible for the observed magnetism in nanowire systems that suffer quantum confinement effects. Our work clearly presents the importance of ordered vacancies internal to nanowires, as well as the effects of dangling bonds about the interface, to the overall magnetization, and points out the fundamental links between local composition, structure and the resulting nanomagnetism.

References

[1] K. Seo, K. S. K. Varadwaj, P. Mohanty, S. Lee, Y. Jo, M. H. Jung, J. Kim, and B. Kim, Nano Lett. **7**, 1240 (2007).

[2] Shih-Wei Hung, Ping-Hung Yeh, Li-Wei Chu, Chii-Dong Chen, Li-Jen Chou, Yi-Jen Wu and Lih-Juann Chen, J. Mater. Chem. **21**, 5704 (2011).

[3] G. Kresse and J. Hafner, Phys. Rev. B **47**, 558 (1993).

[4] Min-Hsiu Hung, Chiu-Yen Wang, Jianshi Tang, Ching-Chun Lin, Te-Chien Hou, Xiaowei Jiang, Kang L. Wang, and Lih-Juann Chen, ACS Nano **6**, 4884 (2012).

[5] Chih-Yen Chen, Yu-Kai Lin, Chia-Wei Hsu, Chiu-Yen Wang, Yu-Lun Chueh, Lih-Juann Chen, Shen-Chuan Lo, and Li-Jen Chou, Nano Lett. **12**, 2254 (2012).

[6] Cheng-Tse Lee, Tzu-Yuan Li, Shian-Haw Chiou, Shen-Chuan Lo, You-Hong Han, and Hao Ouyang, Journal of Applied Physics **113**, 17E140 (2013).

[7] Te-Chien Hou, You-Hong Han, Shen-Chuan Lo, Cheng-Tse Lee, Hao Ouyang, and Lih-Juann Chen, Applied Physics Letters **98**, 193104 (2011).

[8] A.E. van Arkel and J. H. de Boer, Anorg. Allgem. Chem. **148**, 345 (1925).

[9] Yung-Jung Hsu and Shih-Yuan Lu, J. Phys. Chem. B **109**, 4398 (2005).

[10] J.P. Gambino and E.G. Colgan, Materials Chemistry and Physics **52**, 99 (1998).

[11]H. Ouyang, K.-W. Lin, C.-C. Liu, S.-C. Lo, Y.-M. Tzeng, Z.-Y.Guo, and J. van Lierop, Phys. Rev. Lett. **98**, 097204 (2007).

[12] G. Kresse and J. Hafner, Phys. Rev. B **47**, 558 (1993).

[13] G. Kresse and J. Furthmüller, Phys. Rev. B **54**, 11169 (1996).

[14] R. P. Feynman, Phys. Rev. **56**, 340 (1939).

[15] C. L. Kuo, S. Lee and G. S. Hwang, J. Appl. Phys. **104**, 054906 (2008).

[16] T.-K. Liu, C.-T. Lee, S.-H. Chiou, Y.-W. Hsu, J. van Lierop and H. Ouyang, Nanotechology, 26, 065707 (2015).

[17]A. Sundaresan, R. Bhargavi, N. Raangarajan , U. Siddesh and C. N. R. Rao, Phys. Rev. B, 74, 161306 (2006) and J. M. D. Coey, Solid State Sciences, 7, 660 (2005).

[18] D. Shinoda and S. J. Asanabe, J. Phys. Soc. Jpn. **21**, 555 (1966).

[19] Myung-Hwan Whangbo et al., J. Solid State Chem. **176**, 417 (2003).

[20] W.C. Tsai, H.C. Hsu, H.F. Hsu, and L.J. Chen, Applied Surface Science **244**, 115 (2005).

[21] S. P. Murarka, Journal of Vacuum Science & Technology **17**, 775 (1980).

[22] C. H. Luo, G. H. Shen, and L. J. Chen, Applied Surface Science **113/114**, 457 (1997).

[23] N. N. Zhuravlev and A. A. Stepanova, Atomnaya Energiya **13**, 183 (1962).

[24] Zhiqiang Chen, Uroš Cvelbar, Miran Mozeticˇ, Jiaqing He, and Mahendra K.

Sunkara, Chem. Mater. **20**, 3224 (2008).

[25] the Ceder's Materialsproject home page:

https://www.materialsproject.org/materials/mp-18748/

[26] Z. J. Pan, L. T. Zhang, and J. S. Wu,Appl. Phys.101, 0033715(2007)

[27] R.F. Egerton, P. Li and M. Malac, Micron **35**, 399 (2004).

[28] S. Arimoto, M. Sugimura, H. Kageyama, T. Torimoto and S. Kuwabata, Electrochim. Acta **53**, 6228 (2008).

[29] R. J. Bell and P. Dean, Phil. Mag. **25**, 1381 (1972).

[30] R. F. W. Bader, Chemical Reviews, 1991, 91, 893-928.

[31] W. Tang, E. Sanville, and G. Henkelman A grid-based Bader analysis algorithm without lattice bias, J. Phys.: Condens. Matter 21, 084204 (2009).

[32] E. Sanville, S. D. Kenny, R. Smith, and G. Henkelman An improved grid-based algorithm for Bader charge allocation, J. Comp. Chem. 28, 899-908 (2007).

[33] G. Henkelman, A. Arnaldsson, and H. Jónsson, A fast and robust algorithm for Bader decomposition of charge density, Comput. Mater. Sci. 36, 254-360 (2006).

[34] M. Yu and D. R. Trinkle, Accurate and efficient algorithm for Bader charge integration, J. Chem. Phys. 134, 064111 (2011).

[35] S. Caprara, E. Kulatov, and V. V. Tugushev, Eur. Phys. J. B **85**, 149 (2012).

[36] Li Zeng, J. X. Cao, E. Helgren, J. Karel, E. Arenholz, Lu Ouyang, David J. Smith, R. Q. Wu, and F. Hellman, Physical Review B **82**, 165202 (2010).

[37] Soshin Chikazumi, Physics of Ferromagnetism, Oxford University Press, New York, p.125 (1997).

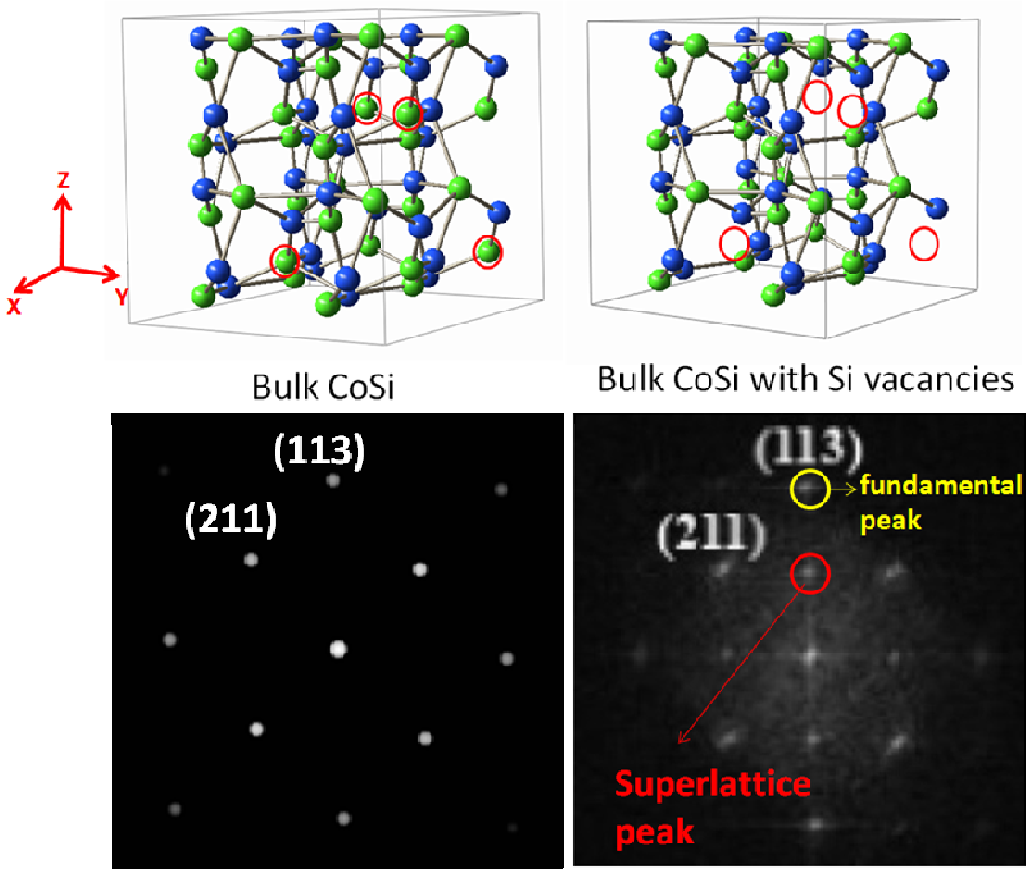

Figure 1 The CoSi structure and the corresponding diffraction pattern. The positions of the Si vacancies are marked with red circles. Blue atoms correspond to Co atoms, green ones correspond to Si atoms, and the red circles correspond to the Si vacancy sites.

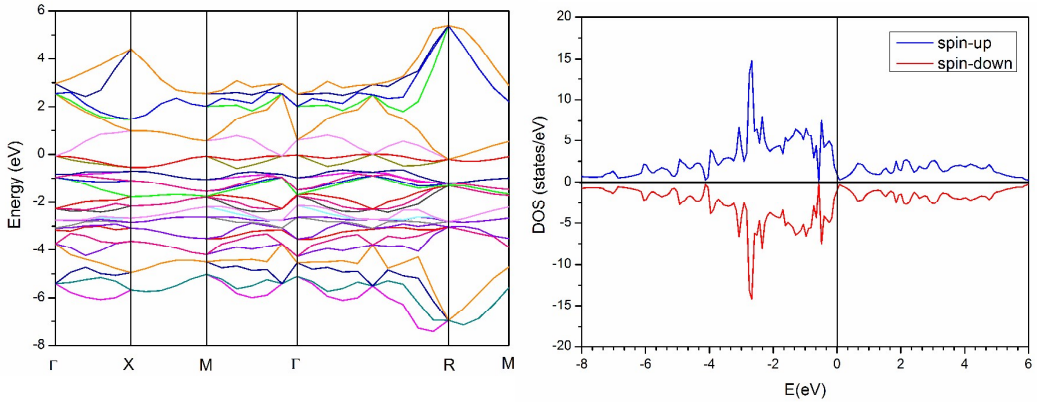

Figure 2 The band structure [25] and corresponding DOS of bulk CoSi [26].

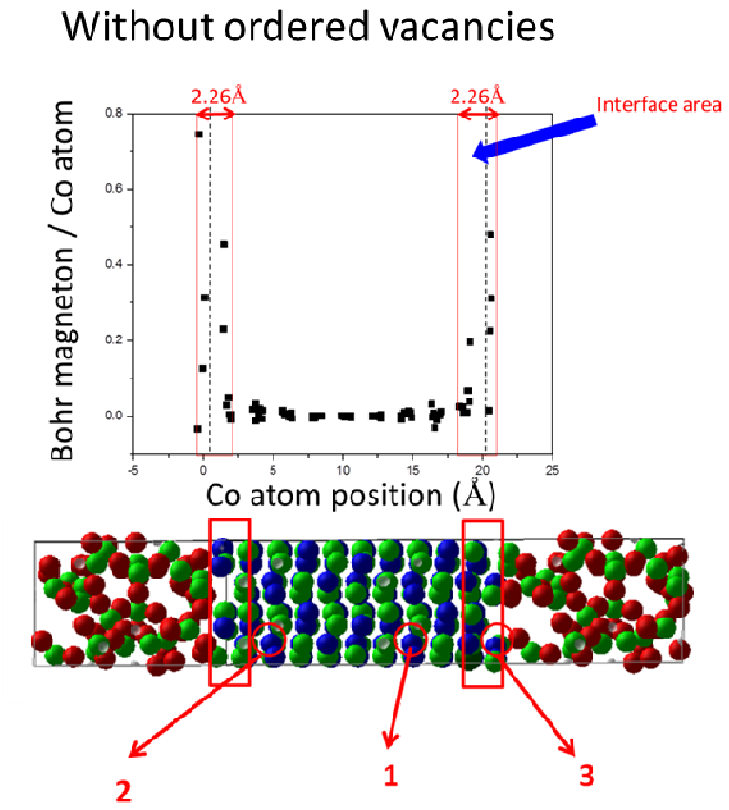

Figure 3 Distribution of simulated moment of Co atoms around SiO_2/CoSi (without ordered vacancies)/SiO_2 interface and the chosen three Co atoms with different distances to the interface.

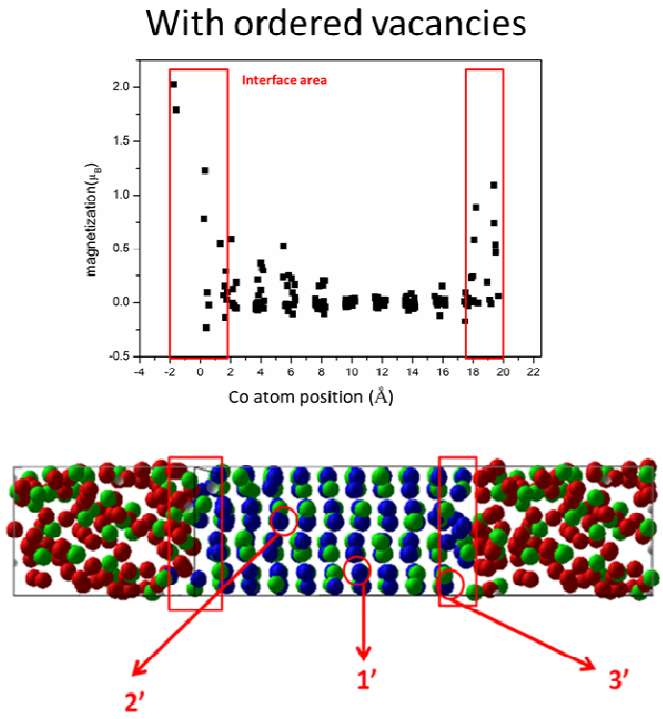

Figure 4 Distribution of simulated moment of Co atoms around SiO_2/CoSi (with ordered vacancies)/SiO_2 interface and the chosen three Co atoms with different distance to the interface.

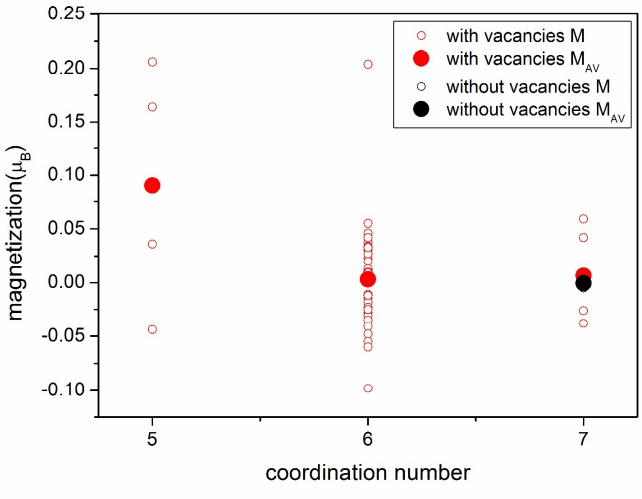

Figure 5 The statistics of internal Co atoms moments from different coordination numbers in both CoSi-SiO_2 configurations, as described in the text.